Current collection by an active spherical electrode in an unmagnetized plasma

E. Ahedo[a] and M. Martínez-Sánchez
Department of Aeronautics and Astronautics, Massachusetts Institute of Technology, Cambridge, Massachusetts 02139

J. R. Sanmartín
E.T.S.I. Aeronáuticos, Univ. Politécnica, Madrid 28040, Spain

(Received 12 July 1991; accepted 16 July 1992)

A theoretical model for the steady-state response of anodic contactors that emit a plasma current I_i and collect electrons from a collisionless, unmagnetized plasma is presented. The use of a (kinetic) monoenergetic population for the attracted species, well known in passive probe theory, gives both accuracy and tractability to the theory. The monoenergetic population is proved to behave like an isentropic fluid with radial plus centripetal motion, allowing direct comparisons with *ad hoc* fluid models. Also, a modification of the original monoenergetic equations permits analysis of contactors operating in orbit-limited conditions. Besides that, the theory predicts that, only for plasma emissions above certain threshold current a presheath/double layer/core structure for the potential is formed (the *core* mode), while for emissions below that threshold, a plasma contactor behaves exactly as a positive-ion emitter with a presheath/sheath structure (the *no-core* mode). Ion emitters are studied as a particular case. Emphasis is placed on obtaining dimensionless charts and approximate asymptotic laws of the current-voltage characteristic.

I. INTRODUCTION

The interaction between a charge-collecting body and a surrounding plasma is a subject of current interest in space engineering. Specific areas of application are spacecraft charge control, electrodynamic tethers, ion thrusters, beam discharges, and artificial clouds. Here, we are interested in the operation of an electrodynamic tether where large electrical currents (~ 10 A) are needed.[1] This requires the use of efficient plasma contactors at both ends of the cable, the electron-collecting contactor, at the anodic end, being the most critical one since the thermal current density of ionospheric electrons is very low (~ 1 mA/m^2). Passive metallic electrodes and thermionic emitters seem unsuitable for those high currents because a contactor of either large area or high impedance is required.[2] On-going laboratory experiments[3–5] suggest that the most promising devices seem to be hollow cathodes, which attain a good electrical contact by emitting a plasma cloud, its external surface acting as an effective collecting area. However, both theory and technology still present gross uncertainties.

On the one hand, a complete theory would have to deal with the simultaneous presence of several difficult phenomena such as the breakdown of quasineutrality, the kinetic formulation generally required to track the species densities, the anisotropy introduced by the geomagnetic field and the motion and geometry of contactor, and the presence of plasma instabilities; meanwhile, theoretical analysis of simplified models, which progressively attack these phenomena, can be illuminating. On the other hand, no real tests have yet been conducted in space, and ground experiments face great difficulties to simulate them.[2,6,7] For a 10 A current, the ionospheric collecting diameter D_{col} is above 25 m at maximum density. Clearly, to avoid wall effects, D_{col} should be, in actual simulation tanks, about two orders of magnitude lower. One thus needs to scale accordingly both Debye length λ_D and electron gyroradius r_e, so as to reproduce the dimensionless numbers $D_{col}/\lambda_D \sim 10^4$ and $D_{col}/r_e \sim 10^3$ which gauge electric shielding and magnetic channeling effects. Actual experiments, however, have values $D_{col}/\lambda_D \sim 200$ and $D_{col}/r_e \sim 20$, typically, very far from reproducing even moderate-current applications. Note, further, that the contactor itself should be similarly scaled. Ground experiments are necessary, nonetheless, to understand the complex physical processes occurring in contactor emissions and to validate the theoretical models.

The seminal work on passive electrodes immersed in unmagnetized plasmas is mainly due to Langmuir and his colleagues,[8–10] who proposed to use the current-voltage (CV) response for plasma diagnosis. Mott-Smith and Langmuir[9] showed that the maximum current a passive probe can collect from a collisionless plasma (the *orbital motion limit*) could be easily deduced from the particle energy and angular momentum conservation laws. Besides that limit, the determination of the current collected from a Maxwellian plasma requires us to solve, first, an integrodifferential equation for the potential. Bernstein and Rabinowitz[11] showed that the problem can be reduced to a differential equation if the attracted species is assumed to be monoenergetic (an idea already considered in Ref. 9). With this assumption, Lam[12] obtained asymptotic solutions for spherical and cylindrical probes. Later,

[a]Present address: E. T. S. I. Aeronáuticos, Ciudad Universitaria, Madrid 28040, Spain.

 0899-8213/92/123847-09$04.00

Laframboise[13] integrated numerically the Maxwellian model and compared it with the monoenergetic one. He found that, for a spherical probe, the agreement was excellent when $R/\lambda_D \gg 1$ (R is the probe radius) and moderate only when $R/\lambda_D \leqslant 1$; for a cylindrical probe the agreement is fairly good for all probe radii. In conclusion, the monoenergetic approximation gives, at least for $R/\lambda_D \gg 1$ (the case we are mainly interested in), a successful balance between tractability and accuracy.

For active electrodes, experiments performed with thermionic emitters by Langmuir and Blodgett[8] showed that the collected current increases when the electrode emits an electrical current of opposite sign, but potential barriers at the electrode surface eventually bound the emitted and collected currents (the *space charge limit*). Both for passive probes and ion emitters, the potential profile is generally constituted by a non-neutral *sheath*, where most of the potential drop occurs, and an outer quasineutral *presheath*. Langmuir found that ionization of an interposed neutral gas can create a quasineutral *core* around the electrode and overcome the space charge limit; the sheath becomes then a *double layer* (i.e., a region with two layers of opposite electrical charge, and vanishing electric field at its edges) separating core and presheath. Double-layer structures are also common in plasma tube discharges, fusion plasmas, and natural space plasmas.[14] Experiments with plasma contactors immersed in unmagnetized, weakly collisional plasmas, suggest the core/double-layer configuration as very suitable.[3–5]

Planar double layers in plasma tube discharges were analyzed by Andrews and Allen[15] using the monoenergetic approximation. Recently, this planar limit has been numerically approached by Katz and Davis[16] with a particular heuristic model. (The planar double-layer theory, which profits from a layer thickness much smaller than the typical scale of the plasma, can treat the layer as a discontinuity surface.) Spherical double layers have been studied by Wei and Wilbur.[17] Their results were included by Gerver *et al.* [7] in a collisionless, double-layer model for spherical contactors. Iess and Dobrowolny[18] studied the presence of double layers in collisional plasmas, using a radial multifluid model that included heuristic collision terms.

We will here complete and extend the model of Gerver *et al.* in several aspects. We intend to (i) use more accurate kinetic models for the plasma species, (ii) apply consistently dimensional and asymptotic techniques, (iii) include the orbit-limited regime, and (iv) obtain a general expression for the CV response of a plasma contactor. Lam's analysis will be mainly used for points (i) and (ii). Point (iii) will require us to modify the original monoenergetic equations of Bernstein–Rabinowitz. Point (iv) is the final objective of the paper and tries to obtain results and conclusions useful for applications.

In Sec. II the model hypotheses and equations are discussed. In Sec. III we integrate Poisson's equation for the potential profile. In Sec. IV we analyze the current-voltage characteristic for the two modes and two regimes that are found. In Sec. V we discuss the work done and compare with other models.

II. FORMULATION OF THE PROBLEM

The plasma contactor is a sphere of radius R, biased to a positive potential V_p relative to an undisturbed ambient plasma of density N_∞. The contactor emits ions (which are accelerated outward) and electrons (which remain confined around the anode), the flow of this emitted plasma being characterized by the ion current I_i. The current-collection problem consists basically in determining the ambient-electron current I_e to the anode as a function of V_p, I_i, R, and the thermodynamic state of the species; alternatively, we take I_e given and determine R. We assume that eV_p is much higher than the thermal energy of all species, and we look for a steady-state solution with no magnetic field effects; also, we include neither collisional nor external ionization processes (the associated mean free paths are too high in the considered applications[7]). The problem then reduces to solving Poisson's equation,

$$\frac{\epsilon_0}{r^2}\frac{d}{dr}\left(r^2\frac{dV}{dr}\right)=e(N_e-N_{ia}+N_{ec}-N_i), \tag{1}$$

where $V(r)$ is the electrostatic potential along the radial distance r to the center of the anode, $N_e(N_{ia})$ is the density of ambient electrons (ions), and N_{ec}, N_i are the corresponding densities of emitted species; ions are positive and singly charged.

Collisionless kinetic theory is used to study the ambient plasma. For $eV_p \gg T_{i\infty}$, where $T_{i\infty}$ is the undisturbed temperature of the ambient ions, N_{ia} is accurately given by the Boltzmann equilibrium law,[12]

$$N_{ia}\simeq N_\infty \exp(-eV/T_{i\infty}), \tag{2}$$

and the number of ions reaching the contactor is negligible. Far from the contactor the attracted species (electrons) is assumed to be monoenergetic with a uniform distribution of angular momentum J; the relation between the undisturbed energy $E_{e\infty}$ and the electron temperature is discussed in Sec. V. Assuming that there is a particular angular momentum J_B, such that electrons with $J<J_B$ are absorbed by the anode while those with $J\geqslant J_B$ are turned back without reaching it, Bernstein and Rabinowitz[11] found that the electron density is (see Appendix A)

$$\frac{2N_e}{N_\infty}=\left(1+\frac{eV}{E_{e\infty}}\right)^{1/2}\pm\left(1+\frac{eV}{E_{e\infty}}-\frac{b_B^2}{r^2}\right)^{1/2}, \tag{3}$$

where $b_B^2\equiv J_B^2/2m_eE_{e\infty}$ is proportional to the current collected:

$$I_e=\pi b_B^2 eN_\infty(2E_{e\infty}/m_e)^{1/2}, \tag{4}$$

and the plus and minus signs are to be used for $r>r_B$ and $r<r_B$, respectively; r_B is given by Eq. (A3).

The right-hand side of Eq. (3) requires that $1+eV/E_{e\infty}\geqslant b_B^2/r^2$. Setting $r=R$, that condition reads $I_e\leqslant I_{eM}$ where I_{eM} turns out to be the orbit-limited current:

$$I_{eM}=\pi b_R^2 eN_\infty(2E_{e\infty}/m_e)^{1/2}$$

$$[b_R^2\equiv R^2(1+eV_p/E_{e\infty})]. \tag{5}$$

In Appendix A we show that once the orbital motion limit is attained, not all the electrons with $J<J_B$ reach the contactor; then Eqs. (3) and (4) are no longer valid and they are to be substituted by

$$\frac{2N_e}{N_\infty}=\left(1+\frac{eV}{E_{e\infty}}\right)^{1/2}+\left(1+\frac{eV}{E_{e\infty}}-\frac{b_R^2}{r^2}\right)^{1/2}-a\left(1+\frac{eV}{E_{e\infty}}-\frac{b_B^2}{r^2}\right)^{1/2}, \tag{3'}$$

$$I_e=I_{eM}; \tag{4'}$$

in Eq. (3'), we have $a=0$ for $r>r_B$ or $r<r_{B'}$, and $a=2$ for $r_{B'}<r<r_B$; $r_{B'}$ is given by Eq. (A4). Note that the current I_{eM} depends on the contactor parameters and is independent of J_B. In the following, for sake of clarity, Eqs. (3) and (4) will be called the *Bernstein–Rabinowitz (BR) regime* and Eqs. (3') and (4') the *orbit-limited (OL) regime.*

For the emitted species we make an analysis similar to the ambient species. Although the exact distribution of confined electrons is difficult to compute, a plausible assumption, supported by experimental data,[4,5,10] is that at least for a steady state, it also corresponds to a Boltzmann equilibrium

$$N_{ec}=N_p\exp[e(V-V_p)/T_{ec}], \tag{6}$$

where the constant N_p will be determined by imposing that the total plasma is quasineutral at least at the contactor surface, and T_{ec} is the (known) electron temperature. For the emitted ions and assuming $E_{ic}\ll eV_p$, where E_{ic} is their kinetic energy when leaving the contactor, we may neglect the angular momentum distribution (as in the Allen–Boyd–Reynolds model for collection of zero-temperature ions by a sphere[19]) because transverse velocities decrease like $1/r$ as the ions move outwards; the expansion is then radial and we have

$$N_i=\frac{I_i}{4\pi r^2 e}\left(\frac{m_i/2}{e(V_p-V)+E_{ic}}\right)^{1/2}. \tag{7}$$

III. THE POTENTIAL PROFILE

Let us first consider a contactor operating in the BR regime (the OL regime will be briefly treated at the end of the section). To obtain the potential profile we have to integrate Eq. (1) together with Eqs. (2)–(4), (6) and (7). As R does nor appear explicitly in the density equations the most straightforward way of integration is from $r=+\infty$ toward $r=R$, considering R, instead of I_e, as the unknown parameter. Far away from the anode there is a region, the *presheath*, where we have $V=O(T_{i\infty})$ and quasineutrality holds; moreover, if

$$I_i m_i^{1/2}/I_e m_e^{1/2}\equiv\mu\ll(eV_p/E_{e\infty})^{1/2} \tag{8}$$

[we will usually have $\mu\leqslant O(1)$], the densities of the emitted species may be neglected there. Then, Eq. (1) becomes $N_e\simeq N_{ia}$ and yields the potential profile $V(r)$,

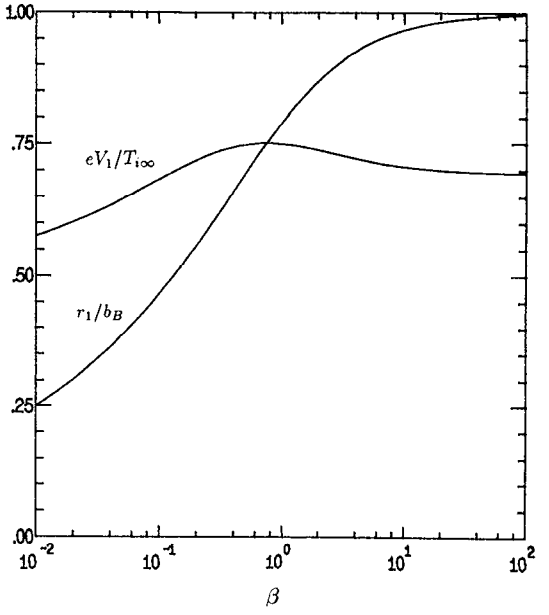

FIG. 1. Sheath outer boundary position r_1 and potential V_1 vs the electron-to-ion temperature ratio $\beta=E_{e\infty}/T_{i\infty}$.

$$\frac{2r}{b_B}=\exp\left(\frac{eV}{T_{i\infty}}\right)\left[\left(1+\frac{eV}{E_{e\infty}}\right)^{1/2}\exp\left(\frac{eV}{T_{i\infty}}\right)-1\right]^{-1/2}. \tag{9}$$

The presheath asymptotically matches with a non-neutral *sheath* around the point $r=r_1$, where $dV/dr\to-\infty$. [It can be proven, from a local analysis of Eq. (1), together with the Bernstein–Rabinowitz hypotheses that lead to Eq. (3), that the transition to the sheath cannot occur at any r different from r_1; therefore, the sheath outer boundary is uniquely determined.] Figure 1 shows r_1/b_B and $eV_1/T_{i\infty}$ versus the parameter $\beta=E_{e\infty}/T_{i\infty}$; for $\beta\ll1$ we have $r_1/b_B\simeq(e\beta/8)^{1/4}$ and $eV_1/T_{i\infty}\simeq\frac{1}{2}+(2\beta/e)^{1/2}$, while for $\beta\gg1$ we have $r_1/b_B\simeq1-\ln 2/2\beta$ and $eV_1/T_{i\infty}\simeq\ln 2+(1-\ln 2)/2\beta$.[12] Notice that the quasineutral approximation for the presheath only requires that $r_1\gg$(Debye length).

The details of the transition layer between presheath and sheath are relevant only locally and they are not needed to pursue the analysis.[12] Inside the sheath, an asymptotic analysis shows that $eV\sim eV_p\gg E_{e\infty}$, the electric field is much higher than outside it, and only the accelerated species (ambient electrons and emitted ions) are important. Also, Eq. (3) for N_e admits the approximation

$$N_e\simeq\frac{I_e}{4\pi r^2 e}\left(\frac{m_e/2}{eV+E_{e\infty}}\right)^{1/2}, \tag{10}$$

as long as $(r_1^2/r^2-1)\ll eV/E_{e\infty}$. This simplified expression for N_e is the only one we will need hereafter because it can be shown that N_e becomes negligible when $b_B^2/r^2\sim eV/E_{e\infty}\gg1$. Now, defining the dimensionless variables

$$F\equiv\left(\frac{32\epsilon_0^2\pi^2 e}{m_e}\right)^{1/3}\frac{V}{I_e^{2/3}},\quad \tau\equiv\frac{r_1}{r},$$

and using Eqs. (1), (7), and (10), the sheath potential $F(\tau)$ fulfills

$$\tau^2 \frac{d^2F}{d\tau^2} \simeq \frac{1}{F^{1/2}} - \frac{\mu}{(F_p - F)^{1/2}}, \tag{11}$$

where μ, Eq. (8), and $F_p \equiv F(V_p)$ are considered known. The appropriate conditions at the sheath outer boundary are

$$\tau = 1^+: \quad F = 0, \quad \frac{dF}{d\tau} = 0. \tag{12}$$

Note that the thermal energy of the species have been consistently neglected in Eq. (11).

The integration of Eqs. (11) and (12) shows that, when τ increases, the electric field $dF/d\tau$ starts increasing from zero, reaches a maximum at $F = F_p/(1+\mu^2)$, and decreases afterward. Depending on the values of μ and F_p, either $dF/d\tau$ becomes zero at certain $F < F_p$ (the *core mode*), or F reaches F_p with $dF/d\tau$ still positive (the *no-core mode*). The transition between modes depends on a function $\mu = \mu_s(F_p)$, later determined, such that the core and no-core modes correspond to $\mu > \mu_s$ and $\mu < \mu_s$, respectively.

A. The core mode

Here, the integration of Eqs. (11) and (12) yields, at the point where $dF/d\tau$ becomes zero, the values $F = F_2(F_p,\mu)$ and $\tau = \tau_2(F_p,\mu)$, wherefrom

$$r_2 = \frac{r_1}{\tau_2(F_p,\mu)}, \quad V_2 = \frac{V_p}{F_p} F_2(F_p,\mu). \tag{13}$$

In this mode, the sheath is actually a *double layer* and point 2 is its inner boundary. Around that point there is a transition from Eq. (11) to the equation

$$N_{ec} - N_i + N_e \simeq 0, \tag{14}$$

and a quasineutral core occupies the region $R < r < r_2$. (The details of this transition are similar to those of point 1.) The potential $V(r)$ inside the core comes out from Eq. (14) together with Eqs. (6), (7), and (10). Particularizing $V(r)$ at $r = r_2$ and $r = R$ we determine N_p in Eq. (6) and the contactor radius,

$$\frac{R^2}{r_2^2} \simeq \left(1 + e\frac{V_p - V_2}{E_{ic}}\right)^{1/2} \exp\left(e\frac{V_2 - V_p}{T_{ec}}\right) \times \frac{\mu - (E_{ic}/eV_p)^{1/2}}{\mu - [(eV_p - eV_2 + E_{ic})/eV_2]^{1/2}}. \tag{15}$$

For the (common) case $V_p - V_2 \ll V_p$, the last factor in Eq. (15) is approximately equal to 1, and the contribution of N_e to Eq. (14) is negligible. Therefore, the core structure depends mainly on the emitted ions dynamics and the confined electrons temperature. (Note, then, that the inclusion of anomalous scattering of the accelerated electrons would scarcely modify the core potential profile.)

Contrary to the double-layer outer boundary (point 1), the inner boundary (point 2) is not singular (i.e., $dV/dr|_2$ is finite); it has been uniquely determined from the condition that the total electric charge inside the double layer is zero. Actually, Eq. (14) presents two singular points for $V(r)$ but both are placed out of the region where it is valid: the first one corresponds to $N_i \simeq N_e$ and is the inflection point of the double-layer potential, Eq. (11); the second one corresponds to $eV \simeq eV_p + E_{ic} - T_{ec}/2$ and, in order to obtain a monotonic profile with $dV/dr < 0$, we must impose the Bohm-like condition

$$E_{ic}/T_{ec} \gg 1/2. \tag{16}$$

B. The no-core mode

The core region vanishes ($r_2 \to R, V_2 \to V_p$) when $dF/d\tau$ becomes zero just at $F = F_p$. The transition curve to the no-core mode, $\mu = \mu_s(F_p)$, can be determined from the implicit equation $F_p = F_2(F_p,\mu)$. Wei and Wilbur[17] computed the relations $\mu_s(F_p)$ and $\tau_p[F_p,\mu_s(F_p)]$; Appendix B treats analytically the asymptotic case $F_p \gg 1$, obtaining for those relations the approximate laws (B3) and (B4).

When $\mu < \mu_s(F_p)$ the sheath extends till the contactor surface and is no longer a double layer ($dF/d\tau|_R > 0$). Now, the integration of Eqs. (11) and (12) yields, at $F = F_p$, a relation $\tau = \tau_p(F_p,\mu)$ and, finally, the probe radius

$$R = r_1/\tau_p(F_p,\mu); \tag{17}$$

the approximate law (B2) for $\tau_p(F_p,\mu)$ is valid in the asymptotic case $F_p \gg 1$. Therefore, in the no-core mode the contactor operates exactly as a positive-ion emitter ($N_{ec} = 0$): the emitted electrons are confined to a thin boundary layer around the contactor and its influence on the global current-voltage response is negligible.

C. The OL regime

The integration of Eq. (1) using now Eqs. (3′) and (4′) for N_e and I_e is similar to the BR regime; in particular both the core and no-core solutions exist. (The mode and the regime a contactor is operating at depends on several parameters, as we discuss in Sec. IV.) In the presheath, the potential is obtained from $N_e \simeq N_{ia}$ [if Eq. (8) holds] and the condition $dV/dr \to \infty$ gives again the sheath outer boundary; both r_1/b_B and $eV_1/T_{i\infty}$ depend now on β and b_B/b_R. [At point B, there is a discontinuity of dV/dr due to the change in factor a of Eq. (3′) for N_e; it can be proven that its effect is small and local.] In the sheath (or in the double layer) the potential $V(r)$ fulfills again Eqs. (11) and (12) *if* μ and F are redefined in the following way:

$$\mu = \frac{(m_i/m_e)^{1/2} I_i}{(2b_B^2/b_R^2 - 1) I_{eM}},$$

$$F = \left(\frac{32\epsilon_0^2 \pi^2 e}{m_e I_{eM}^2}\right)^{1/3} \frac{V}{(2b_B^2/b_R^2 - 1)^{2/3}}.$$

For the core mode, the potential in the core is obtained from Eq. (14) with Eq. (3′) for N_e.

Finally, if the electrode is an *ion emitter* instead of a plasma emitter (i.e., it only emits positive ions, so $N_{ec} = 0$), a quasineutral core cannot be formed, but both the BR and the OL regime may exist. For $\mu < \mu_s(F_p)$, Eq. (17) is valid; the case $\mu = \mu_s(F_p)$ corresponds to the space charge limit,

when the electric field at the emitter surface just becomes zero; and the range $\mu > \mu_s(F_p)$ is unphysical because it leads to nonmonotonic profiles that would turn the emitted ions back to the electrode.

IV. CURRENT-VOLTAGE DIAGRAMS

It is here convenient to use the dimensionless parameters

$$\lambda_D=\left(\frac{\epsilon_0 T_{i\infty}}{e^2 N_\infty}\right)^{1/2}, \quad \chi_p=\frac{eV_p}{T_{i\infty}}, \quad \tilde{\chi}_p=\chi_p\left(\frac{\lambda_D}{R}\right)^{4/3},$$
$$j_m=\beta^{1/2}\frac{b_B^2}{4r_1^2}, \quad j_{e,i}=\frac{I_{e,i}}{4\pi R^2 e N_\infty}\left(\frac{m_{e,i}}{2T_{i\infty}}\right)^{1/2}, \tag{18}$$

so that $\tilde{\chi}_p \equiv F_p j_e^{2/3}$, $j_i \equiv \mu j_e$, and $j_m(\beta)$ is computed with the aid of Fig. 1.[20]

For the *OL regime* the CV characteristic is, in both modes, Eq. (4'); in dimensionless form we have

$$j_e=j_{eM}(\chi_p,\beta)=\frac{\beta^{1/2}+\chi_p/\beta^{1/2}}{4}. \tag{19}$$

[In this regime, the integration of Poisson's equation is only needed to determine the potential $V(r)$ and the ratio b_B/b_R in terms of χ_p, R/λ_D, β, j_i, E_{ic}/T_{ec}, and $T_{ec}/T_{i\infty}$.]

Let us consider now the *BR regime*, where $V(r)$ had to be known prior to determine the CV diagrams. In the *no-core mode* the dimensionless CV characteristic is, from Eqs. (4), (17), and (18), $j_e(\tilde{\chi}_p,\beta,j_i)$:

$$j_e=j_m\tau_p^2(\tilde{\chi}_p/j_e^{2/3}, j_i/j_e). \tag{20}$$

An analytic approximation of this function, valid for thick sheaths ($\tilde{\chi}_p, j_e \gg 1$), is, from Eq. (B5),

$$\tilde{\chi}_p \simeq \frac{A_0}{j_m^{1/2}}\left(j_e^{7/6}-\frac{j_e^{1/2}j_i}{\sigma_s\tilde{\chi}_p^{1/2}}\right)+\frac{3j_i}{4\tilde{\chi}_p^{1/2}}\ln\left(\frac{j_e}{j_m}\right). \tag{21}$$

For zero emission, $j_i=0$, the classical passive anode diagrams are recovered. For $\tilde{\chi}_p$ (and β) fixed and j_i increasing, the total (negative) charge inside the sheath decreases and j_e increases; according to Eq. (21), the effects of the ion emission are significant only when $j_i \gtrsim O(\tilde{\chi}_p)$, roughly. At the transition to the core mode, the sheath total charge vanishes and the values of the emitted and collected currents, $j_{iS}(\tilde{\chi}_p,\beta)$ and $j_{eS}(\tilde{\chi}_p,\beta)$, are obtained from $j_e(\tilde{\chi}_p,\beta,j_i)$ together with $j_i/j_e=\mu_s(\tilde{\chi}_p j_e^{-2/3})$; for the thick sheath limit we have the approximate laws

$$\tilde{\chi}_p \simeq \frac{3\sigma_s}{4}j_{eS}^{2/3}\ln\left(\frac{j_{eS}}{j_m}\right),$$
$$j_{iS}\simeq\frac{3^{1/2}\sigma_s^{3/2}}{2}j_{eS}\left[\ln\left(\frac{j_{eS}}{j_m}\right)\right]^{1/2}. \tag{22}$$

Notice that $j_{iS} \propto \tilde{\chi}_p^{3/2}/\ln\tilde{\chi}_p$, roughly, so the higher $\tilde{\chi}_p$ is, the larger the ion current we require to reach the core mode. Increasing j_i beyond $j_{iS}(\tilde{\chi}_p,\beta)$, the quasineutral core starts developing, moving the double layer away from the anode; in this process the double-layer thickness ratio r_1/r_2 usually decreases. Using Eqs. (4), (13), and (15), the dimensionless CV characteristic for the *core mode* has the functional form

$$j_e=j_e\left(\tilde{\chi}_p,\beta,j_i,\frac{E_{ic}}{T_{ec}},\frac{T_{i\infty}R^{4/3}}{T_{ec}\lambda_D^{4/3}}\right). \tag{23}$$

For j_i high enough, the double layer becomes quasiplanar; then $r_1/r_2 \simeq 1$, $j_i/j_e \simeq (V_p/V_2)^{1/2}+(V_p/V_2-1)^{1/2}$, and the form of the CV characteristic simplifies into

$$j_e=j_e(eV_p/T_{ec},\beta,j_i,E_{ic}/T_{ec}).$$

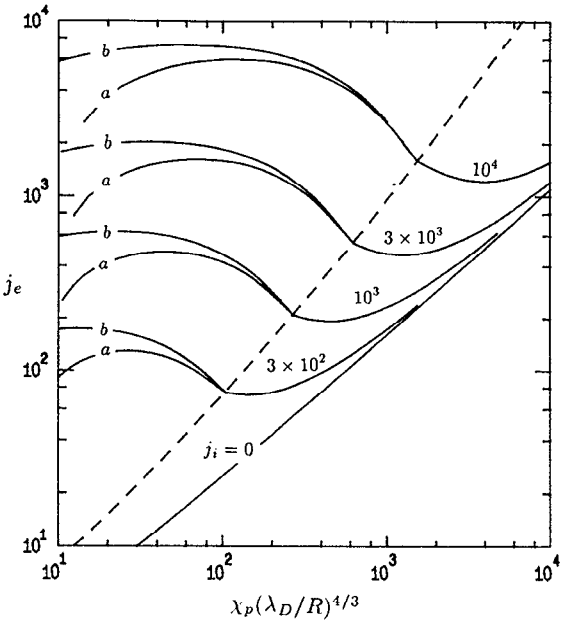

FIG. 2. Dimensionless CV characteristic for $\beta=1.5$, $E_{ic}/T_{ec}=0.5$, $(T_{i\infty}/T_{ec})(R/\lambda_D)^{4/3}$ equal to (a) 1 and (b) 5, and several values of j_i. The curves represent the Bernstein–Rabinowitz regime only, i.e., j_e is assumed to be less than $\chi_p/4\beta^{1/2}$. The dashed line separates the core (left) and no-core (right) modes.

Figure 2 shows j_e versus $\tilde{\chi}_p$ for several values of j_i and $T_{i\infty}R^{4/3}/T_{ec}\lambda_D^{4/3}$; the OL regime has not been included so the curves are valid as long as $j_e \ll j_{eM}$. Whereas j_e always increases with j_i increasing (till reaching the OL value j_{eM}), we observe in Fig. 2 that the variation of j_e with $\tilde{\chi}_p$ is not monotonic except for the passive case. Moreover, the CV response is very different from one mode to the another. While, in the no-core mode, j_e depends mainly on $\tilde{\chi}_p$, in the core mode, j_e is governed by j_i and depends weakly on $\tilde{\chi}_p$. It is found that $j_e \sim j_i(\ln j_i)^{-1/2}$ when the core starts forming and $j_e \sim j_i$ when the core is fully developed. We also observe, from curves (a) and (b) of Fig. 2, that an increase of the core temperature T_{ec} decreases the current collected j_e. The CV response for values of β and E_{ic}/T_{ec} other than those used in Fig. 2 does not present qualitative differences.

In Fig. 3 we have computed the emission current j_i and contactor potential χ_p required to collect several currents j_e (with R/λ_D, β, and $T_{ec}/T_{i\infty}$ fixed). Here, the different functional response for the two modes *and* the two regimes are more dramatically shown. As long as $j_i \ll \tilde{\chi}_p$, the poten-

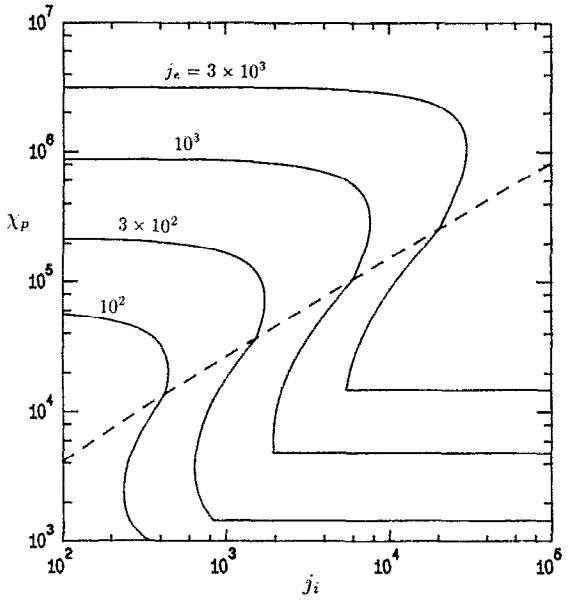

FIG. 3. Emission current j_i and contactor potential χ_p required to collect several electron currents j_e, for $\beta=1.5$, $T_{ec}/T_{i\infty}=100$ and $R/\lambda_D=31.6$ (so $\tilde{\chi}_p \simeq 10^{-2}\chi_p$). The region to the left (right, resp.) of the dashed line corresponds to the no-core (core, resp.) mode. The horizontal segments represent orbit-limited conditions.

tial required is approximately the passive limit value, $\chi_p \sim (R/\lambda_D)^{4/3} j_e^{7/6}$; but, if $O(\chi_p) \ll j_i$, the *same* current j_e can be collected with a potential $\chi_p \sim j_e$ (that means, in Fig. 3, two orders of magnitude less). For $j_i \gg j_e$, the OL regime is reached and j_e, Eq. (19), is independent of j_i.

Figure 4 allows us to determine, in the parametric plane $\chi_p - R/\lambda_D$, whether a plasma contactor reaches the orbital motion limit within the no-core or core modes (the

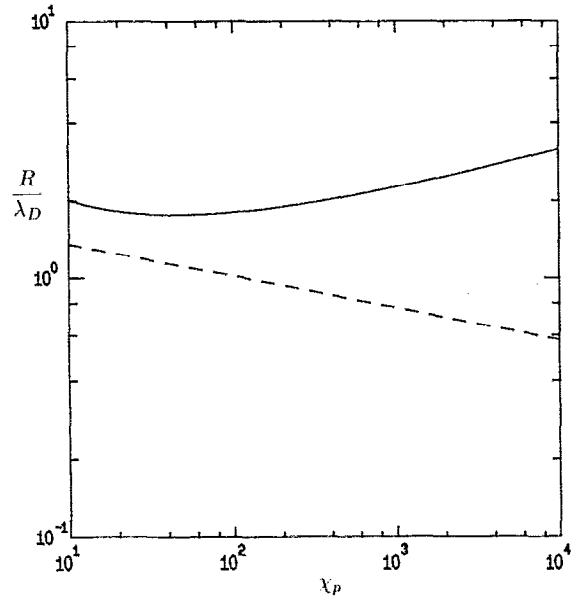

FIG. 4. Different parametric regions for the onset of the orbit-limited regime.

case represented in Fig. 3 corresponds to the last case). The solid line is $j_{eS}(\tilde{\chi}_p,\beta) = j_{eM}(\chi_p,\beta)$, or, using Eqs. (19) and (22),

$$R/\lambda_D \simeq 2^{5/2}(\beta\chi_p)^{1/4}(3\sigma_s \ln \chi_p)^{-3/4}.$$

Above this line, we have $j_{eS} < j_{eM}$, so the OL value is attained once the core is formed; on the contrary, when the contactor parameters lay below the solid line the OL current is attained before the core is formed. Notice that plasma contactors for current-collection applications, which usually have $R \gg \lambda_D$, will collect the OL current in the core mode for all practical values of χ_p. The dash line in Fig. 4 is $j_{eM} = j_e(\tilde{\chi}_p,\beta,j_i=0)$, or, using Eqs. (21) and (22),

$$R/\lambda_D \simeq 2\beta^{5/8}(b_B/A_0 r_1)^{3/4}\chi_p^{-1/8};$$

the parametric domain below this dash line corresponds to electrodes that collect the OL current even in the passive limit, $j_i=0$. This orbit-limited domain was already identified by Laframboise but not by Lam, who incorrectly used Eq. (3) for N_e to study the case $R/\lambda_D \ll 1$. (With the Maxwellian model, a spherical passive probe collects the OL current only in the asymptotic limit $R/\lambda_D=0$.)

Finally, the CV characteristic of an ion emitter ($N_{ec}=0$) is given by Eq. (20) and the space charge limit (dash lines in Figs. 2 and 3) is an upper bound for both the emitted and collected currents; ion emitters are then restricted to

$$j_i \leqslant j_{iS}(\tilde{\chi}_p,\beta), \quad j_e \leqslant \min[\, j_{eS}(\tilde{\chi}_p,\beta), j_{eM}(\chi_p,\beta)\,],$$

so they cannot collect the OL current when they are above the solid line of Fig. 4. Therefore, the space charge upper bound makes ion emitters unsuitable for high-current applications in space.

V. DISCUSSION

We have presented a theoretical model for the steady-state current-voltage response of spherical plasma contactors acting as anodes. Approximate kinetic models have been used for the plasma species. Using standard dimensional analysis and asymptotic techniques, the influence of the various dimensionless parameters on the potential profile and the collection of current have been studied. Both approximate asymptotic laws and numerical charts for the the CV diagrams have been obtained. Results are also applicable to cathodes exchanging V_p by $|V_p|$ and the roles played by ions and electrons.

The theory covers the full range of plasma emissions by the contactor. It also includes ion emitters and passive electrodes as particular cases. The theory predicts that two operating modes exist (for a plasma contactor): when the emission of plasma is low the contactor behaves basically as a positive-ion emitter, the potential profile having a sheath/presheath structure (the no-core mode), while for high plasma emissions the contactor can sustain a quasineutral core (the core mode), separated from the presheath by a double layer. As a consequence, the CV response (in the BR regime) is qualitatively different in

each mode: in the no-core mode the current collected depends mainly on the contactor potential while in the core mode it is basically proportional to the emitted current. We may then conclude that only plasma emitters operating in the core mode can both collect a high current and have a small impedance. The no-core/core modes present strong analogies with the no-ignited/ignited modes observed in some ground-based experiments[4] where a neutral gas cloud surrounds the contactor; the ignited mode corresponds to contactor potentials V_p above some critical value, when the major source of emitted current I_i is the ionization of gas by the electrons accelerated through the double layer; I_i is here governed by the density of neutrals and the double-layer inner potential V_2.

A subject not included in other active electrode theories is the analysis of the OL regime. To our knowledge, Eq. (3') has not previously been treated analytically, even in passive probe theories. The OL regime is, in a certain sense, more relevant for active electrodes than for passive ones, because it covers a broader region in the parametric plane $\chi_p - R/\lambda_D$. For ion emitters the most interesting result is that the collected current is upper bounded either by the orbital motion limit or by the space charge limit, depending mainly on the emitter radius. The OL regime is attainable by plasma emitters of any radius if the emitted current is high enough.

Within the assumed collisionless framework, I_{eM}, Eq. (5), is the maximum current a contactor can collect. The presence of counterstreaming and trapped populations makes possible the onset of streaming instabilities, mainly within the core. In our unmagnetized plasma case, the induced scattering and turbulence could (a) enhance the current collected beyond I_{eM} and (b) favor core thermalization. Then, Eqs. (15) and (23), which determine the core potential and the CV response for the BR regime, could be valid beyond the orbital motion limit (at least while $V_p - V_2 \ll V_p$). In a magnetized plasma, the anomalous scattering is considered essential to enhance cross-field transport and, therefore, the collected current.[7]

Finally, a remarkable point of the monoenergetic model, which we have not mentioned before, is that an algebraic manipulation of Eqs. (3) and (4) yields the following Bernoulli-like equation:

$$\frac{m_e}{2}\left(\dot{r}_e^2+\frac{J_B^2}{2m_e^2r^2}\right)+E_{e\infty}\left(\frac{N_e}{N_\infty}\right)^2-eV=E_{e\infty}\,, \tag{24}$$

where

$$\dot{r}_e=-I_e/4\pi r^2 eN_e$$

is the average electron radial velocity. Hence, a monoenergetic population behaves like an isentropic fluid with radial *plus* centripetal motion; the average angular momentum is $J_B/\sqrt{2}$ and the specific heat ratio is 3, as in the case of electron–plasma waves in a collisionless plasma.[21] Moreover, for Eq. (24) to exactly represent an isentropic fluid equation, the undisturbed electron temperature must be equal to $(2/3)E_{e\infty}$ [this value is slightly smaller than the one proposed by Lam, $(\pi/4)E_{e\infty}$, based on equating *for small potentials* the random thermal current of the monoenergetic and Maxwellian populations]. For the OL regime, there does not exist a simple fluid equivalence because N_e in Eq. (3') depends on the contactor parameters through b_R. Equation (24) proves that *ad hoc* radial fluid models, widely used in the literature, do not recover an essential feature of the particle motion: the reflection of particles with high angular momentum. The consequence is twofold: on the one hand, radial models overestimate the current collected (for instance, the commonly used isothermal model gives a 60% overestimate on j_m), and, on the other hand, they cannot properly recover the OL regime.

ACKNOWLEDGMENTS

This work was supported by Comisión Interministerial de Ciencia y Tecnología of Spain (Project ESP89-0170). The stay of one of the authors (EA) at the Massachusetts Institute of Technology was supported by a Fulbright Scholarship from Spain.

APPENDIX A: EQUATIONS FOR A MONOENERGETIC POPULATION

In the Bernstein–Rabinowitz and Laframboise papers, the equations for a monoenergetic population were obtained particularizing the general solution for a multienergetic population. A simple, direct derivation of those equations is presented here, for the case of a monotonic potential profile. According to Bernstein and Rabinowitz, the density and current of a monoenergetic population are

$$\frac{N_e(r,\chi)}{N_\infty}=\int_0^{b_m(R)}\frac{bdb/2r^2}{(1+\chi/\beta-b^2/r^2)^{1/2}}+\int_{b_m(R)}^{b_m(r)}\frac{bdb/r^2}{(1+\chi/\beta-b^2/r^2)^{1/2}}\,, \tag{A1}$$

$$I_e=eN_\infty(2E_{e\infty}/m_e)^{1/2}\pi b_m^2(R), \tag{A2}$$

where $\chi\equiv eV/T_{i\infty}$, $b=J(2m_eE_{e\infty})^{-1/2}$ (b is the impact parameter), and the function $b_m(r)$ is defined as the minimum value of $b_r(r')=r'[1+\chi(r')/\beta]^{1/2}$ in the domain $r'>r$. The first integral in Eq. (A1) is the density of electrons in transit to being captured by the (perfectly absorbing) anode, while the second integral corresponds to those that are turned back at some radius between R and r, the "reflected" electrons.

Since $b_r\to\infty$ as $r\to\infty$, one has $db_r/dr'<0$ at large r'. If a sheath develops at some point [where $\chi(r')$ steepens sharply], $b_r(r')$ will exhibit a minimum b_B at a nearby point r_B that fulfills

$$1+\chi(r_B)/\beta-b_B^2/r_B^2=0. \tag{A3}$$

Hence, we have $b_m(r)\leqslant b_B$ for $r<r_B$ and, at least, *two regimes* exist corresponding to b_B being higher or smaller than $b_r(R)=b_R\equiv R(1+\chi_p/\beta)^{1/2}$ (Fig. 5). [Additional regimes can exist if $b_r(r')$ has more minima.] When $b_m(R)=b_B<b_R$ [Fig. 5(a)] one sets, in Eqs. (A1) and (A2), $b_m(r)$ equal to $b_B[b_r(r)$,resp.] for $r<r_B[r>r_B$,resp.] and obtains Eqs. (3) and (4). For some parametric do-

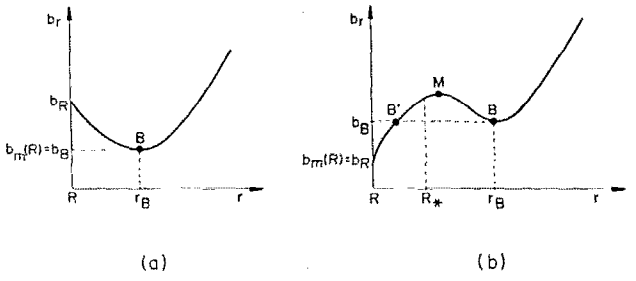

FIG. 5. Impact parameter function $b_r(r)=r[1+\chi(r)/\beta]^{1/2}$ with a single minimum at point B. (a) Bernstein–Rabinowitz regime: electrons with $b\leqslant b_B$ are captured by the probe; an electron with an impact parameter $b>b_B$ is reflected back at the point where $b_r(r)=b$. (b) Orbit-limited regime: electrons with $b\leqslant b_R$ are captured; "free" electrons with $b>b_R$ are reflected back in the region $r>r_B$ or the region $R<r<r_{B'}$; "trapped" electrons with $b_B\leqslant b\leqslant b_r(r)$ may exist in the region $r_{B'}<r<r_B$.

main, and in particular for small enough R when all other parameters are fixed, we find $b_m(R)=b_R<b_B$ [Fig. 5(b)]. We then have $b_m(r)$ equal to $b_B[b_r(r)$,resp.] for $r'_B<r<r_B$ [$r>r_B$ or $r<r'_B$, resp.], with $r_{B'}$ given by

$$b(r_{B'})=b_B\,, \tag{A4}$$

and Eqs. (A1) and (A2) yield Eqs. (3′) and (4′). In this second regime electrons are not turned back by intermediate barriers so we have reached orbit-limited conditions.

In the orbit-limited regime, Eqs. (3′) and (4′), there may exist electrons trapped in orbits of finite range (less than, or equal to, $r_B-r_{B'}$) for values b such that $b_B<b<b_r(r_M)$, where r_M is the radius for the relative maximum M [Fig. 5(b)]. Trapped electrons may also exist in the first regime, for a probe radius [such as R_* in Fig. 5(b)] less than r_M. As one decreases R, a trapped population may first appear when the maximum M occurs at the probe $db_r/dr|_R=0$,

$$\beta+\chi+\frac{r}{2}\frac{d\chi}{dr}=0 \quad \text{at} \quad r=R. \tag{A5}$$

[Integration of Eq. (11) shows that, for passive electrodes, trapped particles may exist for sheath radii $r_1>2.4R$, instead of $r_1>1.3R$ given by Lam.[22]] Bernstein and Rabinowitz limited their analysis to $R>r_M$ to avoid treating the trapped particles problem; they consequently did not reach the orbit-limited regime. Laframboise considered both regimes (and several ones for the Maxwellian model) but trapped particles were always neglected. In our theory, trapped electrons have been assumed part of the confined electron population.

APPENDIX B: SHEATH ASYMPTOTIC SOLUTIONS

Equations (11) and (12) can be treated analytically in two limits: $F_p\ll 1$ (*thin sheath*) and $F_p\gg 1$ (*thick sheath*). In the applications we are considering the thin sheath limit appears in the core mode when I_i is high enough, while the thick sheath limit appears in the no-core mode at high V_p and low I_i.

The *thin (or quasiplanar) sheath* solution is well known:[14]

$$\tau(F,F_p,\mu)=1+F_p^{3/4}\int_0^{F/F_p}[x^{1/2}+\mu(1-x)^{1/2}-\mu]^{-1/2}\,dx. \tag{B1}$$

In the no-core mode the parametric relation $\tau_p(F_p,\mu)$ is obtained setting $F=F_p$ in Eq. (B1) (one has $\tau_p\sim F_p^{3/4}\ll 1$). The mode transition occurs at $\mu=\mu_s(F_p)\simeq 1$. In the core mode, imposing that $F=F_2$ and $\tau=\tau_2$ at $dF/d\tau|_2=0$, we obtain, first,

$$\frac{F_2(F_p,\mu)}{F_p}=\frac{4\mu^2}{(1+\mu^2)^2}$$

and then, integrating Eq. (B1), $\tau_2(F_p,\mu)$.

We will here derive the asymptotic solution for a *thick sheath* in the no-core mode. Calling $\sigma\equiv\mu F_p^{-1/2}$, Eq. (11) gives $F(\tau,F_p,\sigma)=A(\sigma)\tau+O(\sigma\ln\tau)$ when $\tau\gg 1$, the (positive) function $A(\sigma)$ being computed by integrating (11) from $\tau=1$ with conditions (12). Hence, at dominant order, the electric field is Coulombian and proportional to $A(\sigma)$. The numerical integration shows that the linear approximation $A(\sigma)=A_0(1-\sigma/\sigma_s)$ with $A_0=1.9$ and $\sigma_s\simeq 2.1$ is good enough for practical calculations. This yields

$$F_p\simeq\left(1-\frac{\mu}{\sigma_s F_p^{1/2}}\right)A_0\tau_p+O\left(\frac{\mu\ln\tau_p}{F_p^{1/2}}\right) \tag{B2}$$

as an implicit equation for $\tau_p(F_p,\mu)$; for $\mu=0$ we recover the classical passive anode results.[8,12] The sheath becomes a double layer when $A\to 0$, that is, when

$$\mu=\mu_s(F_p)\simeq\sigma_s F_p^{1/2}, \tag{B3}$$

and the $O(\ln\tau_p)$ term in Eq. (B2) needs then to be calculated. As $\mu_s\sim F_p^{1/2}$, the first term of the right-hand side of Eq. (11) is only important for $F\leqslant O(1)\ll F_p$, so, except for a boundary layer around $\tau=1$ of thickness $\Delta\tau=O(1)$, the potential profile is obtained integrating

$$\tau^2\frac{d^2F}{d\tau^2}\simeq-\frac{\sigma_s}{(1-F/F_p)^{1/2}}$$

from $\tau=\tau_p$ toward $\tau=1$. The boundary conditions at $\tau=\tau_p$ are $F=F_p$, $dF/d\tau=0$. The asymptotic solution for $\tau_p-\tau\gg 1$ is[8]

$$\frac{2F_p}{3\sigma_s}\left(1-\frac{F}{F_p}\right)^{3/2}=\ln\left(\frac{\tau_p}{\tau}\right)+\frac{1}{3}\ln\left[\ln\left(\frac{\tau_p}{\tau}\right)\right]+O(1).$$

Setting now $F=0$ at $\tau=1$, we obtain a relation between F_p and τ_p,

$$2F_p\simeq 3\sigma_s\ln\tau_p\,. \tag{B4}$$

A comparison of Eqs. (B3) and (B4) with the numerical results of Wei and Wilbur[17] shows that these analytical approximations give an error of less than a 5% for $F_p\geqslant 20$. Finally, we propose the patching law

$$F_p\simeq\left(1-\frac{\mu}{\sigma_s F_p^{1/2}}\right)A_0\tau_p+\frac{3\mu}{2F_p^{1/2}}\ln\tau_p \tag{B5}$$

to easily approximate $\tau_p(F_p,\mu)$ in the complete range $0\leqslant\mu\leqslant\sigma_s F_p^{1/2}$.

[1]M. Martínez-Sánchez and D. E. Hastings, J. Astronaut. Sci. **35**, 75 (1987).
[2]It has been recently shown that the anodic part of a tether, if uninsulated, could efficiently serve itself as electron collector, making an anodic contactor unnecessary (J. R. Sanmartín, M. Martínez-Sánchez, and E. Ahedo, "Bare wire anodes for electrodynamic tethers," to appear in J. Propulsion Power).
[3]M. J. Patterson and R. S. Aadland, in *Space Tethers for Science in the Space Station Era* (Compositori, Bologna, 1988), p. 261.
[4]P. Wilbur and T. Laupa, Adv. Space Res. **8**, 221 (1988).
[5]G. Vannaroni, M. Dobrowolny, E. Melchioni, F. De Venuto, and R. Giovi, J. Appl. Phys. **71**, 4709 (1992).
[6]I. Katz and V. A. Davis, in Ref. 3, p. 241.
[7]M. J. Gerver, D. E. Hastings, and M. R. Oberhardt, J. Spacecraft **27**, 391 (1990).
[8]I. Langmuir and K. B. Blodgett, Phys. Rev. **24**, 49 (1924).
[9]H. M. Mott-Smith and I. Langmuir, Phys. Rev. **28**, 727 (1926).
[10]I. Langmuir, Phys. Rev. **33**, 954 (1929).
[11]I. Bernstein and I. Rabinowitz, Phys. Fluids **2**, 112 (1959).
[12]S. Lam, Phys. Fluids **8**, 73, 1002 (1965).
[13]J. Laframboise, Ph.D. thesis, University of Toronto, 1966; cited in P. M. Chung, L. Talbot, and K. J. Touryan, *Electric Probes in Stationary and Flowing Plasmas: Theory and Application* (Springer, New York, 1975), p. 14.
[14]M. A. Raadu, Phys. Rep. **178**, 25 (1989); L. Block, Astrophys. Space Sci. **55**, 59 (1978).
[15]J. G. Andrews and J. E. Allen, Proc. R. Soc. London Ser. A **320**, 459 (1971).
[16]I. Katz and V. A. Davis, Phys. Fluids B **1**, 2121 (1989).
[17]R. Wei and P. Wilbur, J. Appl. Phys. **60**, 2280 (1986).
[18]L. Iess and M. Dobrowolny, Phys. Fluids B **1**, 1880 (1989).
[19]J. E. Allen, R. L. Boyd, and P. Reynolds, Proc. Phys. Soc. B **70**, 297 (1957).
[20]The definitions of $j_{e,i}$ and j_m differ in a factor $(1+\beta)^{1/2}/4$ from those used in Ref. 12.
[21]L. Spitzer, *Physics of Fully Ionized Gases* (Wiley, New York, 1962).
[22]As a condition for the setup of trapping, Lam did not use Eq. (A5), appropriate for a monoenergetic population [in Ref. 11, Eq. (8.6) with $E_G=E_{e\infty}$]; instead he used a condition that corresponds to a multienergetic population, Eq. (8.8) of Ref. 11.